Proc. Natl. Acad. Sci. USA
Vol. 93, pp. 14349–14354, December 1996
Applied Biological Sciences

A fusion pore phenotype in mast cells of the ruby-eye mouse

ANDRES F. OBERHAUSER* AND JULIO M. FERNANDEZ†‡

†Department of Physiology and Biophysics, 1-159 Medical Sciences Building, Mayo Clinic, Rochester, MN 55905; and *University of Chile and Centro de Estudios Científicos de Santiago, Casilla 16443, Santiago 9, Chile

Communicated by Bertil Hille, University of Washington, Seattle, WA, October 25, 1996 (received for review July 15, 1996)

ABSTRACT **Using patch-clamp capacitance and amperometric techniques, we have identified an exocytotic phenotype that affects the function of the fusion pore, the molecular structure that connects the lumen of a secretory vesicle with the extracellular environment during exocytosis. Direct observation of individual exocytotic events in mast cells from the ruby-eye mouse (*ru*/*ru*) showed a 3-fold increase in the fraction and duration of transient fusion events with respect to wild-type mice. The fraction of the total fusion events that were transient increased from 0.22 ± 0.02 (wild type) to 0.65 ± 0.02 (*ru*/*ru*), and the average duration of these events increased from 418 ± 32 ms (wild type) to 1207 ± 89 ms (*ru*/*ru*). We also show that this phenotype can reduce and delay an evoked secretory response by causing the fusion of vesicles that have been previously emptied by repeated cycles of transient fusion. The exocytotic phenotype that we describe here may be a cause of diseases like platelet storage pool deficiency and prolonged bleeding times for which the ruby-eye mouse serves as an animal model. Furthermore, the identification of the gene causing the fusion pore phenotype reported here will illuminate the molecular mechanisms regulating exocytotic fusion.**

The earliest event in exocytosis is the formation of a fusion pore, an aqueous channel that connects the lumen of a secretory granule with the extracellular space. The molecular structure of the exocytotic fusion pore is unknown, though its electrical properties have been extensively studied with the patch-clamp technique (reviewed in refs. 1–4). These studies have shown that the fusion pore opens abruptly with an initial conductance that varies between 35 and 1000 pS (5, 6). After opening, the fusion pore can expand in a fluctuating manner to a conductance that exceeds 10 nS, leading to full fusion. Alternatively, the fusion pore can close completely after fluctuating in the open state for hundreds of milliseconds (5, 7–9). Thus, rather than being an irreversible expanding structure, the fusion pore can open and close, finely regulating the amount of secretory products being released. The exocytotic fusion pore likely serves as a key point for the regulation of hormone and neurotransmitter release (3, 10, 11). Therefore, one of the most outstanding questions on the mechanism of exocytotic secretion is the understanding of the molecular structure of the fusion pore.

A complex cascade of protein–protein interactions define the synaptic vesicle cycle (12). Molecular cloning of synaptic vesicle proteins and the identification of the substrates of the botulinum and tetanus neurotoxins have advanced our understanding of the proteins that regulate vesicle docking and fusion. Conserved families of proteins have been found to be associated with vesicle fusion events, from yeast to mammalian cells, and in intracellular traffic as well as in regulated secretion (13–15). This confluence of fields suggests that the molecular structures that regulate membrane fusion are conserved. In spite of these remarkable advances, none of the vesicular or membrane proteins that are thought to regulate vesicular fusion have been shown to be directly involved in the opening or closure of the exocytotic fusion pore.

In an effort to identify the molecular components that regulate the activity of fusion pores, we have studied the kinetics of the fusion pores that form in mast cells from pigment mutant mice, which are known to carry secretory defects (16–19). Mast cell secretory phenotypes can be examined, at high resolution, with the patch-clamp capacitance technique (7). The technique consists of measuring the cell membrane capacitance, which is directly proportional to the cell membrane surface area. Upon fusion of a secretory vesicle, the cell membrane area increases stepwise by an amount equal to the granule membrane area. The step increase in capacitance also marks the opening of the fusion pore. Owing to their large secretory granules (0.2–5 μm) and their well defined secretory products (heparin, histamine, and serotonin), mast cells are an ideal cell type to monitor exocytosis. We monitor the release of secretory products by measuring the oxidation of electroactive substances (e.g., serotonin) with a carbon fiber microelectrode placed near the cell (e.g., ref. 20). This experimental arrangement is capable of resolving the fusion of single secretory vesicles with the plasma membrane and the resulting release of serotonin from the same vesicles. The combination of these two techniques permits the examination of the activity of individual fusion pores. Hence, any secretory phenotype associated with the pigment mutation can be readily detected.

Pigment mutations in mice, like pearl, light ear, ruby-eye, and maroon, are known to affect the exocytosis of melanosomes, lysosomes, and platelet-dense granules. It has been shown that the phenotypes associated with these pigment mutations may also appear in peritoneal mast cells. For example, the phenotype of the beige mouse (bg^j/bg^j) is very large melanosomes. Similarly, peritoneal mast cells obtained from the beige mouse contain very large secretory granules, greatly facilitating the electrophysiological recordings of fusion pores (11, 21). However, thus far, no mouse mutant with abnormalities in the properties of the exocytotic fusion pore have been described. Here we describe, in the ruby-eye mouse, the first phenotype directly associated with the exocytotic fusion pore. We have found that mast cells isolated from ruby-eye mutant mice show a 3-fold increase in the fraction and duration of transient fusion events. The ruby-eye mouse may prove valuable as an animal model to study the molecular basis of fusion pore intermediates, such as those that occur in transient fusion events.

MATERIALS AND METHODS

Preparation of Mast Cells. Mast cells from normal mice (C57BL/6J) and ruby-eye (JE/Le *a*/*a f*/*fje*/+ *ru*/*ru* or JE/Le *a*/*a f*/*fje*/*je ru*/*ru*; The Jackson Laboratory) were obtained by peritoneal lavage. The standard extracellular solution used contained 130 mM NaCl, 2 mM $MgCl_2$, 2 mM $CaCl_2$, and 10 mM Hepes at pH 7.2. The internal solution contained 140 mM

The publication costs of this article were defrayed in part by page charge payment. This article must therefore be hereby marked "*advertisement*" in accordance with 18 U.S.C. §1734 solely to indicate this fact.

‡To whom reprint requests should be addressed. e-mail: fernandez.julio@mayo.edu.

potassium glutamate, 7 mM $MgCl_2$, 0.2 mM Mg-ATP, 10 mM Hepes (pH 7.2), 10 mM EGTA, 1 mM $CaCl_2$, and 3–5 μM GTPγS.

Measurement of Membrane Capacitance. Exocytosis was monitored by measuring the cell membrane capacitance using the whole cell mode of the patch-clamp technique (22) in conjunction with a digital phase detector (23). The phase was periodically adjusted using the phase tracking technique (24) so that one output reflected changes in the real part of the cell admittance (Re [ΔY]), and the second output reflected changes in the imaginary part of the admittance, (Im [ΔY]). These parameters were captured with a temporal resolution of 9.6 ms per point.

Amperometric Detection of Serotonin Release. Amperometric detection of secretory products was monitored with a carbon fiber electrode as described elsewhere (20, 25).

RESULTS

Measurements of changes in cell membrane capacitance caused by the fusion of a secretory granule make it possible to obtain time-resolved measurements of the opening of individual fusion pores and their subsequent dilation or closure. Therefore, any modification of the gene products that determine fusion pore function should be easily detectable by measuring the kinetics of single fusion events in patch-clamped mast cells.

Fig. 1 shows a comparison of the changes in cell membrane capacitance measured in mast cells isolated from normal (Fig. 1*A*) or ruby-eye (Fig. 1*B*) mice. The cells were stimulated by 3 μM GTPγS contained in the pipette solution (7). These recordings were obtained during the initial phase of the degranulation, when the rate of fusion is low and individual fusion events are clearly resolved.

Fig. 1*A* shows two types of events: irreversible step increases in membrane capacitance and transient increases in capacitance (marked by asterisks). The former represents the abrupt and irreversible opening of the fusion pore, whereas the latter represents the opening and subsequent closure of the fusion pore. There are 19 irreversible fusions and 3 transient fusion events. The net increase in cell membrane capacitance during the length of this recording (162 s) was $\approx$180 fF. Membrane capacitance recordings done in mast cells from the ruby-eye mouse are markedly different (Fig. 1*B*). The most striking feature is the large number of transient fusion events. During the 193 s shown, there are >48 transient fusion events and only $\approx$15 irreversible fusion events. The net increase in membrane capacitance during this period was 223 fF. It is difficult to evaluate the exact number of transient fusion events in these traces, since there are many overlapping events. For instance, the group of events marked by a circle could have been originated by three or more (up to six) secretory granules undergoing transient fusion. This problem becomes more evident in later phases of the degranulation, where the rate of fusion is several times faster. To obtain a mean value for the fraction of fusion events that are transient, we calculated this fraction at different times during the degranulation. For this, we counted the number of transient fusion events and the number of irreversible fusion steps in short recording segments (50 s), as shown in Fig. 1*B*. Due to the large number of overlapping fusion events, we could analyze only up to four segments during a degranulation. Fig. 2*A* shows a histogram of the fraction of the total number of fusion events that are transient measured in 18 mast cells. For comparison, the fraction of transient fusion events measured in 16 control mast cells is also shown.

The fraction of transient fusion events measured in mast cells from ruby-eye mice was $\approx$3 times larger than in control cells (0.65 $\pm$ 0.02 and 0.22 $\pm$ 0.02, respectively). The dwell time of the transient fusion events was also increased in the mast cells of the ruby-eye mouse. This parameter was measured in transient fusion events that were clearly due to the fusion of a single secretory granule (like the events shown in Fig. 2*B*). As the histogram in Fig. 2*B* shows, the average duration of transient fusion events is $\approx$3 times longer in ruby-eye mast cells than in control cells. The transient fusion event mean dwell times were 1207 $\pm$ 89 ms (n = 256) in ruby-eye mouse mast cells and 418 $\pm$ 32 ms (n = 167) in control cells.

This large increase in the number and duration of transient fusion events in ruby-eye mouse mast cells does not significantly affect the rate of the degranulation triggered by intracellular perfusion with GTPγS. After a variable delay from the beginning of the whole-cell configuration (11 $\pm$ 1 min; n = 18), the membrane capacitance started to increase at a rate that was similar to that measured in control cells. The rise time of the degranulation, defined as the time between 20% and 80% of the total increase in cell membrane capacitance due to the fusion of all the cell's secretory granules, was 155 $\pm$ 26 s (n =

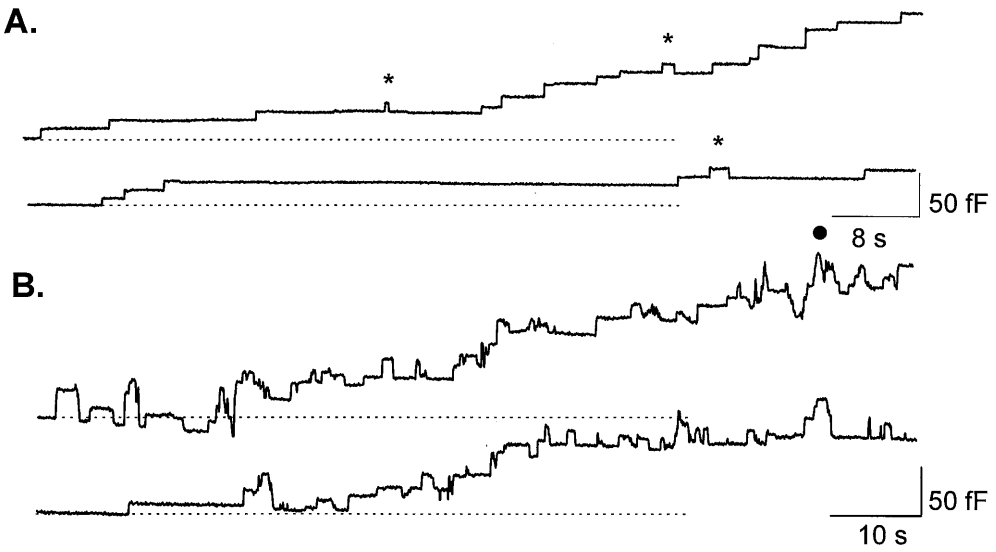

FIG. 1. Mast cells isolated from the ruby-eye mutant mouse show a large increase in the number of transient fusion events. Step changes in cell membrane capacitance that occur during the degranulation of mast cells isolated from wild-type mice (*A*) and ruby-eye mice (*B*). The traces are from a continuous record (total of 2.7 min in *A* and 3.2 min in *B*) during the initial phase of the degranulation. The transient fusion events in *A* are indicated by (*). The degranulation was triggered by adding 3 μM GTPγS to the patch-pipette solution.

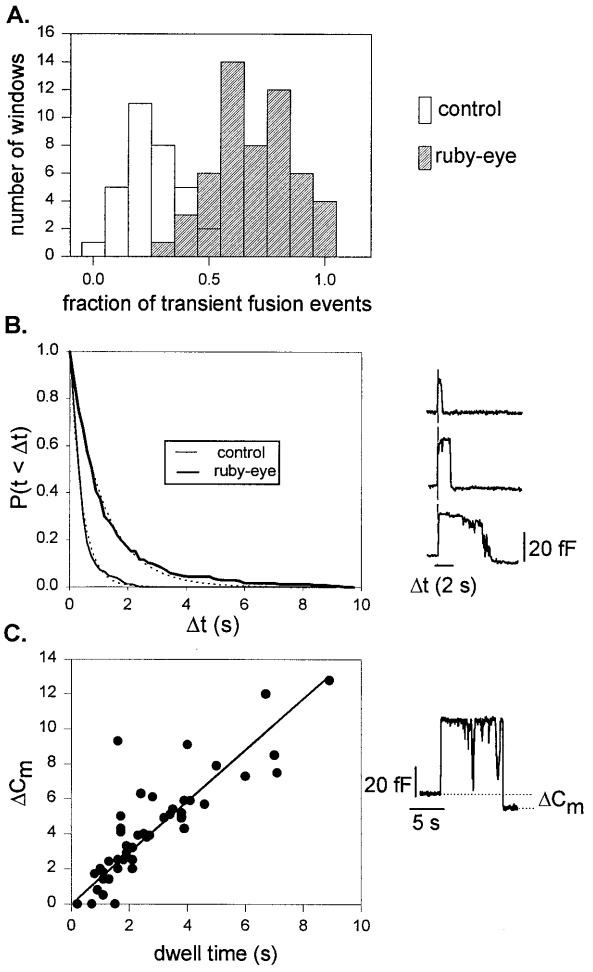

FIG. 2. Analysis of the transient fusion events in ruby-eye mouse mast cells. (*A*) Histogram of the fraction of transient fusion events measured in mast cells obtained from ruby-eye (solid bars) and normal (open bars) mice. The fraction of the total fusion events was calculated from 50-s long segments (at least three per cell) where single fusion events were well-separated (i.e., the initial phase of the degranulation). The mean value was 0.22 ± 0.02 (16 cells, 167 transient fusion events, and 592 irreversible fusion events) in normal mast cells and 0.65 ± 0.02 (18 cells, 258 transient fusion events, and 137 irreversible fusion events) in ruby-eye mast cells. (*B*) Probability distribution functions of the duration of transient fusion events measured in ruby-eye (thick line) and normal (thin line) mouse mast cells. Exponential fits of the distributions (dotted lines) gave time constants of 1100 ms (in ruby-eye mouse mast cells) and 400 ms (in normal mouse mast cells). The measured time constants were similar to the means: 1207 ± 89 ms (in ruby-eye cells, $n = 256$, range = 20–9100 ms) and 418 ± 32 ms (in control cells, $n = 167$, range = 20–2130 ms). (*Right*) Some examples of transient fusion events measured in mast cells from the ruby-eye mouse. (*C*) The rate of lipid flow through the fusion pore is not affected in ruby-eye mouse mast cells. As in the control mast cells, the transient fusion events observed in ruby-eye show a difference in membrane capacitance (*Right*). The time dependence of the decrease in cell capacitance following a transient fusion was 1.46 fF/s (solid line; $n = 49$). This rate of membrane uptake is similar to that reported for wild-type and beige mouse (bg^j/bg^j) mast cells.

11) and 118 ± 32 s ($n = 8$) in ruby-eye and normal mouse mast cells, respectively. These values are not significantly different. In addition, the extent of the degranulation (expressed as the ratio of the final and initial membrane capacitance) is similar in mast cells isolated from mutant or control animals (≈2.5 times; ref. 26). These observations suggest that the granules that fuse transiently with the cell membrane eventually undergo full fusion.

During transient fusion events, the fusion pore connects the plasma membrane with the granular membrane creating a pathway through which a large flow of lipids occurs. Analysis of transient fusion events in mast cells from normal or beige mice revealed that during transient fusion, the stepwise decrease in capacitance observed upon closure of the fusion pore was typically larger than the step increase observed upon its opening, indicating a net transfer of membrane from the cell membrane to the secretory granule membrane (8). Furthermore, the magnitude of this membrane uptake was time dependent, with a slope of 1.6 fF/s corresponding to $\approx 10^6$ lipids per s moving through the fusion pore from the plasma membrane toward the granule membrane. The large lipid flow suggested that the granule membrane was under tension and that the fusion pore was mostly lipidic when it closed (8). The lipid flow through an open fusion pore is likely to be a sensitive parameter of the fusion pore size and structure. We have found that the transient fusion events observed in ruby-eye also showed a difference in the size of the capacitance step caused by the opening and the closing of the fusion pore (Fig. 2*C*; see also Fig. 2*B*) and that this membrane uptake was linearly related to the duration of the transient fusion event (plot in Fig. 2*C*), with a slope of 1.46 fF/s ($n = 49$; $r = 0.72$). This shows that the rate of lipid flow through the fusion pore is not affected in ruby-eye mouse mast cells, suggesting that the mechanisms that determine the closure of the fusion pore do not affect the structural components of the fusion pore that determine the magnitude of the lipid flow.

The fraction of fusion events that are transient in mast cells from the ruby-eye mouse is higher during the initial phase of a degranulation. Fig. 3*A* shows the time course of the cell membrane capacitance increase measured during a complete degranulation of a ruby-eye mouse mast cell. The *Insets* in Fig. 3*A* show an expansion of the membrane capacitance recording at different times during the degranulation. It can be seen that the fraction of fusion events that are transient was higher in the lower left *Inset* (0.89) than in the *Inset* on the right (0.28). Fig. 3*B* (■) shows that the fraction of transient fusion events decreased from 0.65 ± 0.02 ($n = 18$ cells) in the initial phase (<20% of degranulation) to 0.39 ± 0.02 ($n = 16$ cells) at the end of the degranulation (>80% of degranulation). This decrease in the fraction of transient fusion events during the degranulation was not seen in normal mouse mast cells (●).

In mast cells, exocytosis occurs in the compound mode (26, 27). When a secretory granule fuses with the plasma membrane, it provides a path for other granules, deeper in the cell, to fuse and release their secretory products. Thus, the results shown in Fig. 3 suggest that, in ruby-eye mouse mast cells, the secretory granules that are closer to the plasma membrane tend to undergo more transient fusions than the granules that are deeper in the cell. Alternatively, we have suggested that the closure of the fusion pore is dependent on the presence of a particular type of membrane lipid that favors pore closure (9). If the concentration of such lipids was increased in the plasma membrane of the ruby-eye mouse, a higher frequency of fusion pore closure would occur, as observed. Upon degranulation, the large expansion of the plasma membrane would dilute these lipids decreasing the frequency of pore closures.

It has been reported that platelets isolated from the ruby-eye mouse show a large decrease in the content of serotonin in dense granules (by ≈90%; ref. 18). To test if the serotonin levels in mast cells are also affected, we measured the release of serotonin from individual secretory granules during exocytosis by using a carbon fiber in the amperometric mode (11, 20, 28). Fig. 4 shows a combined membrane capacitance (upper traces) and amperometry (lower traces) measurement of exocytosis in a ruby-eye mouse mast cell. It is evident that a significant number of fusion events during the initial phase of the degranulation do not have an associated amperometric spike. This is better seen by integrating the amperometric

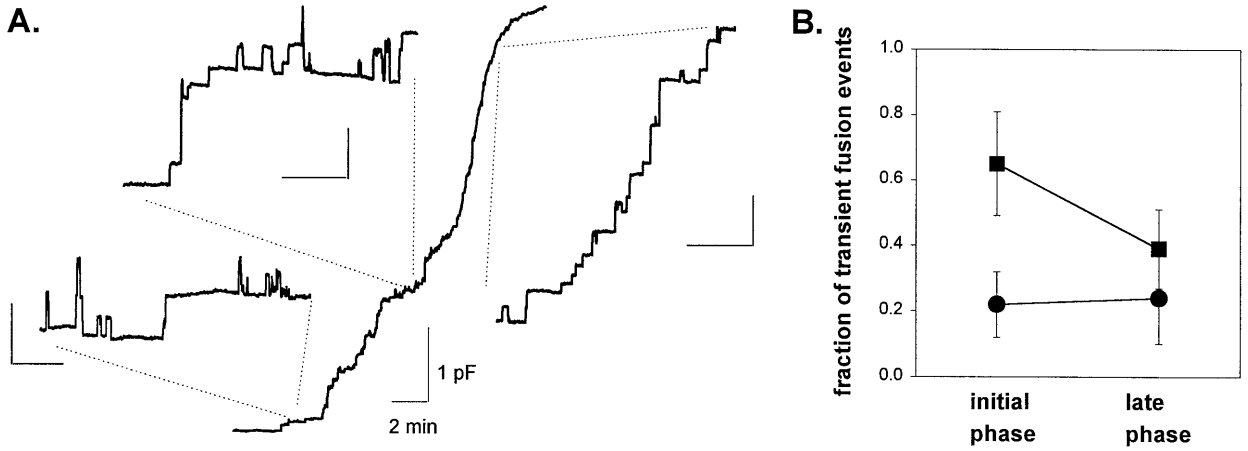

FIG. 3. The incidence of transient fusion events in ruby-eye mouse mast cells is higher during the initial phase of the degranulation. (*A*) Time course of the cell membrane capacitance increase measured during a complete degranulation in a ruby-eye mouse mast cell. The recording starts 5 min after perfusing the cell with 3 μM GTPγS. The cell membrane capacitance increased from 3.7 to 9.9 pF. The rate of degranulation, measured between 20% and 80% of the final capacitance value, was 0.5 pF/min. (*Insets*) Expansion of the membrane capacitance recording at different times during the degranulation. The calibration bars in the insets are 50 fF and 10 s. (*B*) The fraction of fusion events that are transient is higher in the initial phase than at the end of the degranulation in mast cells from the ruby-eye mouse (■). The fraction of transient fusion events was 0.65 ± 0.02 (n = 18 cells) in the initial phase (<20% of total increase in capacitance) and 0.39 ± 0.03 (n = 16 cells) at the end of the degranulation (>80% of total increase in capacitance). In contrast, the fraction of transient fusion events in control mice did not change: 0.22 ± 0.02 (n = 16 cells) for the initial phase and 0.24 ± 0.05 (n = 12 cells) for the late phase (●).

recording over the duration of the membrane capacitance recording. The time integral of the amperometric current (thin line) is delayed with respect to the increase in membrane capacitance. The delay measured at 50% of the degranulation was ≈70 s in this cell. However, this delay was variable and, in some cells (two of five), there was no delay between the integral of the amperometry and the capacitance. The delay between the increase in capacitance and the increase in the integral of the released serotonin is due to the fusion of secretory granules that contain very low levels of serotonin. It is likely that the high frequency of transient fusion events observed in the ruby-eye mice may have also taken place before the patch clamping of the cells. In this case, granules that have fused transiently may have been depleted of their serotonin. Furthermore, as shown in Fig. 3, most of the transient fusion events occur on the early part of a degranulation. Similarly, most of the serotonin depletion is observed in the early phase of a degranulation (Fig. 4), whereas during the later phases, exocytotic release of serotonin appears normal.

It has been shown that preincubation of mast cells with 10 μM serotonin for up to 1 h before an experiment increases the serotonin contents of mast cell secretory granules (11). As Fig. 5 shows, preincubation of mast cells with serotonin restores the secretory granule contents, where fusion events, either transient or irreversible, had an associated spike of serotonin release. After preincubation with serotonin, the time integral of the amperometric current can be superimposed to macroscopic membrane capacitance recording in all the cells studied (n = 5). This result shows that the ruby-eye mouse is competent for serotonin uptake and storage. Furthermore, these results suggest that the fusion events observed in the early phase of the degranulation of ruby-eye mast cell represent the exocytosis of a pool of granules (probably the cortical granules) that have been depleted of serotonin due to several rounds of transient fusion events.

DISCUSSION

We have found that mast cells isolated from ruby-eye mice show a large increase in the fraction and duration of transient fusion events. This novel phenotype should prove useful in understanding the molecular basis of the activity of exocytotic fusion pores. However, we do not know the origin of the fusion pore phenotype observed in ruby-eye mice. Since the *ru/ru* mice bred by The Jackson Laboratory, JE/Le *a/a f/f je/+ ru/ru*, are from a different genetic background than the control mice C57BL/6J (*a/a*), it remains uncertain whether the fusion pore phenotype is related to the different strain, JE/Le vs. C57BL/6J, or to the spontaneous mutations *f/f* (flexed tail) and *ru/ru* (ruby eye). Unfortunately, The Jackson Laboratory does not maintain active mice colonies that can serve as genetic controls for the ruby-eye mouse. In spite of these difficulties, it is likely that the observed fusion pore phenotype is due to a spontaneous mutation in the *ru* gene, since mutations in this gene have been found to be associated with an alteration in the exocytosis of dense granules in platelets and melanosomes in melanocytes (16–19). The eventual molecular cloning of the *ru* gene will help in resolving this issue. This gene has been mapped to a region of the mouse chromosome 19 that includes pale ear (*ep*) and brachymorphic (*bm*) genes (29). Interestingly, all of these pigment dilution genes cause platelet storage pool deficiency and prolonged bleeding times (18). It is not known whether other secretory cells, beside melanocytes, platelets, and mast cells from ruby-eye mice, show a defect in exocytosis. However, it is likely that this mutation is not expressed in neurons, since the ruby-eye mice do not show an obvious alteration in behavior.

We also do not know the mechanism by which the altered gene products expressed in ruby-eye mast cells affect the properties of the exocytotic fusion pore. The observed increase in the incidence of transient fusion events in patch-clamped mast cells may be due to alterations in the proteinaceous "scaffold" that is thought to link the two fusing membranes (2, 3). Indeed, It has been recently shown that mutations in the hemagglutinin scaffold that mediates viral fusion can cause a fusion phenotype where the fusion pore is arrested at a putative hemifusion stage (30). However, the dilution effects shown in Fig. 3 argue against a defect in the proteinaceous scaffold of the fusion pore, since it is likely that all fusion pores would be equally affected by a mutation. In contrast, we observe that the increased fraction of transient fusion events is reduced as a degranulation progresses.

Another possible target of an altered gene product, we speculate, is the lipid composition of the plasma membrane. There is strong evidence suggesting that when the fusion pore

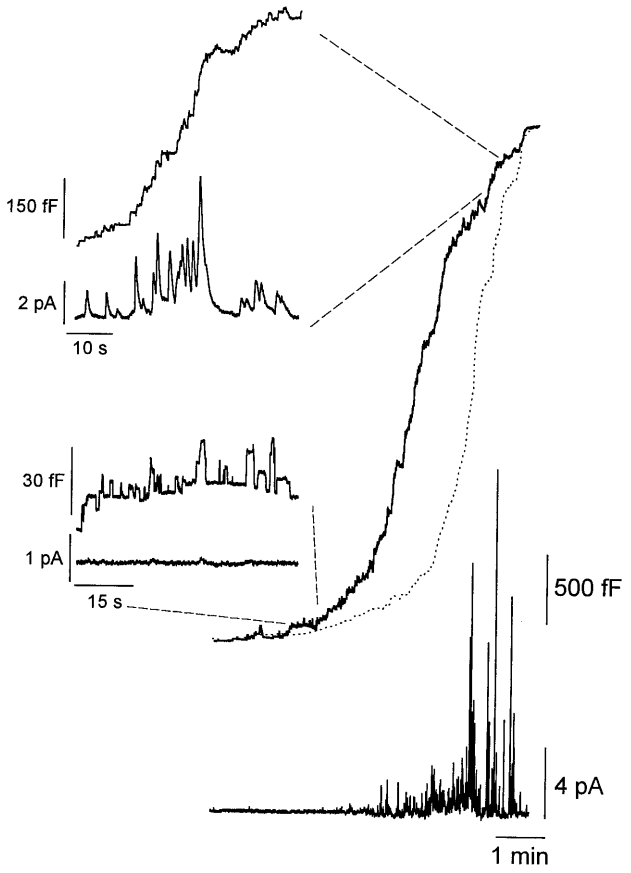

FIG. 4. In ruby-eye mouse mast cells, most of the fusion events seen during the initial phase of the degranulation show little or no release of serotonin. Simultaneous cell membrane capacitance and amperometric measurements of exocytosis in mast cells obtained from ruby-eye mice. The upper traces show the cell membrane capacitance increases during a complete degranulation. The lower traces show the corresponding spike like amperometric recordings of serotonin release. The time integral of the amperometric trace is shown as a dotted line superimposed on the cell membrane capacitance trace and represents the total amount of serotonin detected by the carbon fiber during the secretory response. Secretion was stimulated by adding 5 μM GTPγS to the patch-pipette solution.

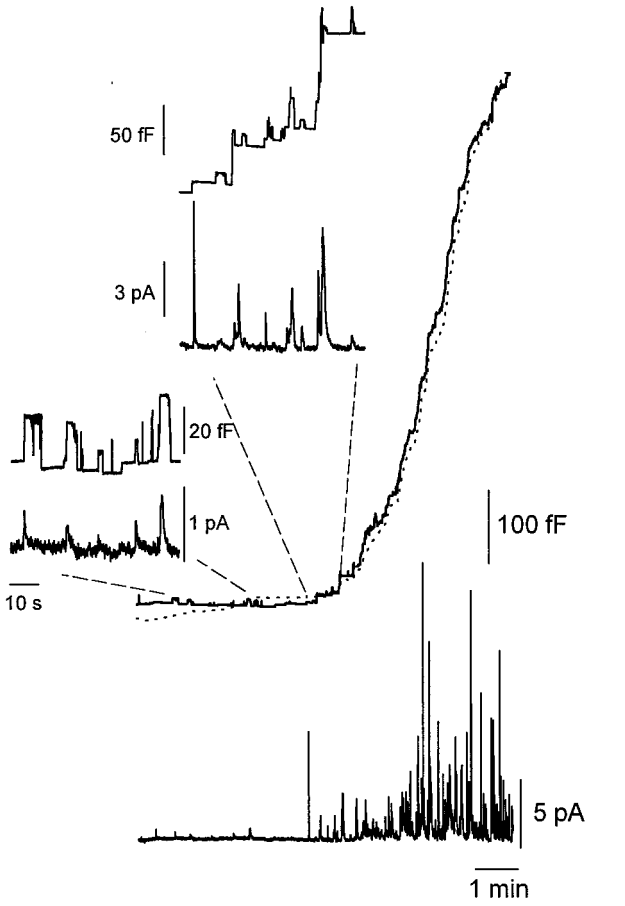

FIG. 5. Preincubation of ruby-eye mouse mast cells with an extracellular saline containing 10 μM serotonin restores the early secretory response. After 1 h of incubation, the mast cell was patch-clamped with a pipette solution containing 5 μM GTPγS. As in Fig. 4, the upper recordings correspond to the membrane capacitance and the lower traces are the amperometric recordings. The dotted line corresponds to the integral of the amperometric trace.

closes, it is mostly made of lipids. For example, when a fusion pore connects a secretory granule to the plasma membrane, there is a large flow of lipids ($\approx 10^6$ lipid molecules per s) into the secretory granule (8), enough to replace all the phospholipids in a small lipidic fusion pore every millisecond. Mathematical modeling of the energetics of a small lipidic pore showed that their probability of closure is dominated by the spontaneous curvature of the constituent lipids (31). Hence, closure of the fusion pore can be triggered by slight changes in the lipid composition of the pore. In support of this view was the finding that the temperature dependence of the rate of closure of the fusion pore was discontinuous at 13°C, suggesting the abrupt phase separation of a lipid that favors pore closing (9). Thus, an alteration in the lipid composition of the plasma membrane, with an increased concentration of a closure favoring lipid, provides a simple mechanism to explain the increase in the probability of fusion pore closure observed in mast cells from ruby-eye mice. Since it is likely that the lipids that regulate fusion pore closure reside in the plasma membrane, the incidence of transient fusion events would be expected to decrease during a degranulation. The massive fusion of the secretory granules into the plasma membrane will decrease the concentration of the closure favoring lipid and the incidence of transient fusion events (as shown in Fig. 3).

Alternatively to the lipid dilution model, it is possible that in ruby-eye mast cells the cortical cytoskeleton is modified in such a manner as to increase the fraction of transient fusion events. Mast cell exocytosis proceeds in a compound mode where peripheral granules fuse first with the plasma membrane and then exocytosis is continued inward by granule–granule fusion (26, 27). Hence, we expect that only the fusion of peripheral granules would be affected by a defective cortical cytoskeleton, explaining the observed phenotype. However, at present, there is no evidence that the transient fusion events observed during exocytosis are regulated by the cortical cytoskeleton.

The large increase in the fraction and duration of the transient fusion events in the mast cells from the ruby-eye mouse is likely to have physiological consequences. We found that during the initial phase of the degranulation, most of the fusion events showed little or no release of serotonin, in contrast with the large amperometric spikes that were associated with the fusion events in later phases of the degranulation. The early release events correspond to the fusion of cortical granules that have been depleted of serotonin due to several rounds of transient fusion events. A similar depletion of secretory products may occur *in vivo*. For example, it has been previously shown that platelets isolated from ruby-eye mice have reduced serotonin levels in dense granules (18, 32). It is possible that a reduced contents of platelet secretory products, caused by an increased frequency of spontaneous transient fusion, is a cause of platelet storage pool deficiency and

prolonged bleeding times. However, we do not yet know whether the fusion pore phenotype that we have observed in mast cells occurs in platelets.

The gene products affected by the pigment mutations are still unknown. However, since several pigment mutants are models of human disorders, such as the Chediak–Higashi syndrome and platelet storage pool deficiency, intense efforts to clone and identify these genes are underway (29, 33). The identification of the gene products responsible for the phenotypes found in the ruby-eye mouse will be significant, because they will illuminate the molecular mechanisms regulating the closure of the fusion pore.

We wish to thank Cindy Camrud for her expert secretarial assistance. This work was supported by the National Institutes of Health (R01 Grants GM 38857 and GM 46688 to J.M.F.), the Mayo Foundation, and by Fondo Nacional de Investigación Científica Tecnológica (Grant 1950437 to A.F.O.).

1. Almers, W. (1990) *Annu. Rev. Physiol.* **52,** 607–624.
2. Monck, J. & Fernandez, J. (1992) *J. Cell. Biol.* **119,** 1395–1404.
3. Monck, J. & Fernandez, J. (1994) *Neuron* **12,** 707–716.
4. Lindau, M. & Almers, W. (1995) *Curr. Opin. Cell Biol.* **7,** 509–517.
5. Spruce, A., Breckenridge, L., Lee, A. & Almers, W. (1990) *Neuron* **4,** 643- 654.
6. Lollike K., Borregaard, N. & Lindau, M. (1995) *J. Cell. Biol.* **99,** 99–104.
7. Fernandez, J. M., Neher, E. & Gomperts, B. D. (1984) *Nature (London)* **312,** 453–455.
8. Monck, J. R., Alvarez de Toledo, G. & Fernandez, J. M. (1990) *Proc. Natl. Acad. Sci. USA* **87,** 7804–7808.
9. Oberhauser, A., Monck, J. R. & Fernandez, J. M. (1992) *Biophys. J.* **61,** 800–809.
10. Chow, R. H., von Ruden, L. & Neher, E. (1992) *Nature (London)* **356,** 60–63.
11. Alvarez de Toledo, G., Fernandez-Chacon, R. & Fernandez, J. M. (1993) *Nature (London)* **363,** 554–557.
12. Südhof, T. C. (1995) *Nature (London)* **375,** 645–653.
13. Bennett, M. K. & Sheller, R. H. (1993) *Proc. Natl. Acad. Sci. USA* **90,** 2559–2563.
14. Söllner, T., Whiteheart, S. W., Brunner, M., Erdjument-Bromage, H., Geromanos, S., Tempst, P. & Rothman, J. E. (1993) *Nature (London)* **362,** 318–324.
15. Calakos, N. & Scheller, R. (1996) *Physiol. Rev.* **76,** 1–29.
16. Novak, E. & Swank, R. T. (1979) *Genetics* **92,** 189–204.
17. Novak, E., Wieland, F., Jahreis, G. & Swank, R. (1980) *Biochem. Genet.* **18,** 549–561.
18. Novak, E., Hui, S.-W., & Swank, R. (1984) *Blood* **63,** 536–544.
19. Gross, S. K., Shea, T. & McCluer, R. H. (1985) *J. Biol. Chem.* **260,** 5033–5039.
20. Oberhauser, A. F., Robinson, I. & Fernandez, J. M. (1996) *Biophys. J.* **71,** 1131–1139.
21. Breckenridge, L. J. & Almers, W. (1987) *Proc. Natl. Acad. Sci. USA* **84,** 1945–1949.
22. Hamill, O. P., Marty, A., Neher, E., Sakmann, B. & Sigworth, F. J. (1981) *Pflügers Arch.* **391,** 85–100.
23. Joshi, C. & Fernandez, J. (1988) *Biophys. J.* **53,** 885–892.
24. Fidler, N. & Fernandez, J. M. (1989) *Biophys. J.* **56,** 1153–1162.
25. Kawagoe, K. T., Zimmerman, J. B. & Wightman, R. M. (1993) *J. Neurosci. Methods* **48,** 225–240.
26. Alvarez de Toledo, G. & Fernandez, J. M. (1990) *J. Gen. Physiol.* **95,** 397–409.
27. Rohlich, P., Anderson, P. & Uvnas, B. (1971) *Acta Biol. Acad. Sci. Hung.* **22,** 197–213.
28. Leszczyszyn, D. J., Jankowski, J. A., Viveros, H., Diliberto, E., Near, J. A. & Wightman, R. M. (1990) *J. Biol. Chem.* **265,** 14736–14737.
29. O'Brien, E. P., Novak, E. K., Keller, S. A., Poirier, C., Guenet, J. L. & Swank, R. T. (1994) *Mamm. Genome* **5,** 356–360.
30. Kemble, G. W., Danieli, T. & White, J. M. (1994) *Cell* **76,** 383–391.
31. Nanavati, C., Markin, V. S., Oberhauser, A. F. & Fernandez, J. M. (1992) *Biophys. J.* **63,** 1118–1132.
32. Paigen B., Holmes, P., Novak., E. & Swank, R. (1990) *Arteriosclerosis (Dallas)* **10,** 648–652.
33. Barbosa, M. D. F., Nguyen, Q. A., Tchernev, V. T., Ashley, J. A., Detter, J. C., Blaydes, S. M., Brandt, S. J., Chotal, D., Hodgman, C., Solari, R. C. E., Lovett, M. & Kingsmore, S. F. *Nature (London)* **382,** 262–265.